EUVE Observations of the Hyades Giants

NASA Contract P.O. S-92503-Z

Final Report

Submitted To:

National Aeronautics and Space Administration
Goddard Space Flight Center
Greenbelt MD 20771

Principal Investigator:

Robert A. Stern
Dept H1-12 Bldg 252
Lockheed Martin Solar and AStrophysics Laboratory
3251 Hanover St.
Palo Alto, CA 94304
(650) 424-3272

September 30, 1998

1. Summary

We describe EUVE and ROSAT observations of the Hyades K0 III giants θ^1 (vB 71=HR1411) and γ (vB 28=HR1346) Tau. We also discuss ASCA observations of θ^1 Tau. The coronal activity of these "clump" giants is intermediate between that of the Sun and of high activity stars such as RS CVn systems. There is no evidence for significant short or long term variability up to several years. Modeling of the individual and combined spectra suggest that these two X-ray and EUV-bright Hyades giants resemble in their activity levels another clump giant, β Cet, with a peak in the emission measure distribution near log T $\sim$ 6.8, reminiscent of the Capella emission measure "bump."

2. Introduction

The Hyades is a unique astrophysical laboratory: at a distance of only $\approx$ 45 pc from the Sun, the Hyades age, mass distribution, and abundances are well known, making it a critical calibration point for all stellar evolution studies using open clusters. Equally important is the Hyades role in our understanding of stellar coronal evolution and the nature of the magnetic dynamo in stars younger than the Sun (see Stern, Schmitt, and Kahabka 1995 and refererences therein). Among the stars in the Hyades are the four K0 III "clump" giants, helium burning stars of $\gtrsim$ 2.2 $M_\odot$. The Hyades giants are perhaps the most extensively studied objects of their kind in any open cluster (e.g. Gilroy 1989). The Hyades giants and dwarfs have been extensively studied at ground-based observatories, and their photospheric abundances are well-determined (Lambert and Ries 1981, Cayrel *et al.* 1985, Griffin and Holweger 1989, Ruck and Smith 1993). The metallicity for the Hyades giants is log [Fe/H]=+0.15 compared to the Sun, and C and O are under-abundant by about 0.4 dex (Lambert and Ries 1981, Cayrel *et al.* 1985, Griffin and Holweger 1989).

The Hyades giants all exhibit chromospheric and coronal activity (see Table 1; Baliunas, Hartmann, and Dupree 1983, Stern *et al.* 1992, and Stern, Schmitt, and Kahabka 1995). Residing in the "clump" region of the H-R diagram, the Hyades giants are also important as they lie near the coronal "dividing line" separating stars with strong and weak (or no) X-ray emission (see Haisch *et al.* 1991 and references therein). At present, the only other example of such a "clump" giant observed by EUVE is the nearby star β Cet (Ayres *et al.* 1998). A major unresolved question is whether the coronal temperature structure and abundance pattern displayed by this star is typical, or if there is a wide variation among the giants themselves. The evolutionary status of such field stars is not nearly as well known as for the cluster giants. Hence to understand the EUV characteristics of these giants as a group, and how they fit into the overall picture of post-main sequence coronal evolution, we need to observe stars with known ages, masses, and compositions, such as the Hyades giants. The Hyades giants also represent a critical link in our unraveling of the Capella system, the nearby binary (G0 III + G 8 III) that has been observed extensively with EUVE (Dupree *et al.* 1993, Brickhouse *et al.* 1995, Dupree *et al.* 1995, Brickhouse 1995).

The four Hyades giants present an intriguing puzzle. Optically, they are nearly indistinguishable from each other: all are spectral type K0 III (ϵ Tauri is occasionally given a G9.5 III classification), and have V-R colors within 0.02 mag (Baliunas, Hartmann, and Dupree 1983; Gilroy 1989). Yet two of the giants (θ^1 and γ Tauri) are 20-50 times brighter in X-rays than the other two , δ and ϵ. In this respect, the two groups of Hyades giants may have an analog in the dichotomy between the giants β Cet and β Gem, which lie quite near each other in the H-R diagram, yet β Cet has an X-ray luminosity $\approx$ 100 times that of β Gem (see discussion in Eriksson *et al.* 1983). With X-ray luminosities of $\approx 10^{30}\ erg\, s^{-1}$, θ^1 and γ Tauri are, in fact, even brighter in X-rays than the most active Hyades G-dwarf, vB 50 (Stern *et al.* 1992, Stern, Schmitt, and Kahabka 1995). θ^1 Tau is known to have a wide binary companion, which is likely an early M dwarf (Griffin and Gunn 1977). However, the typical X-ray luminosity of a Hyades M dwarf is $\approx$ 1% of the X-ray luminosity of θ^1 Tau: it is thus very unlikely that the binary companion contributes significantly to the system's coronal activity (Stern *et al.* 1992). In addition, correlation with chromospheric activity including Mg II fluxes (see Table 1) suggests strongly that the optically faint binary companion is not the source of θ^1 Tau's coronal emission.

The coronally active Hyades giants are also well within the sensitivity range of the EUVE spectrometers: θ^1 Tau was detected in the Al/C filter in the RAP survey at 35 c/ksec (McDonald *et al.* 1994): although this flux is most likely from the He II 304 Å line, it could also contain a contribution from the Fe IX-XI lines at 170–180 Å. Because the giants vary in X-ray luminosity by less than a factor of two over a decade (Stern, Schmitt, and Kahabka 1995), show no evidence of flaring or other short time-scale variability, and have rotation periods $\sim$ 140 days (Baliunas *et al.* 1991), observing the Hyades giants, even at different epochs, allows us to combine EUVE and other data sets for a full picture of the star's emission measure distribution from 10^5–10^8 K.

2.1 Capella and the Hyades Giants

. Capella is a binary system (104 d period) composed of a G8 III primary, a "clump" giant of nearly the same mass as the Hyades giants (Pilachowski and Sowell, 1992) , and a rapidly rotating, G0 III secondary, believed to be a Hertzsprung gap star. Because EUVE cannot resolve the individual components of the system, using the EUV characteristics of a Hyades giant as a "stand-in" for the Capella primary should help in resolving the current controversy regarding the identification of the Capella components with features in the Capella emission measure distribution (DEM). Dupree *et al.* (1993) and Brickhouse *et al.* (1995) noted a "bump" in Capella's DEM near log T $\approx$ 6.8, presumably the result of enhanced Fe XVIII-XIX line emission. Is such a "bump" the result of a composite binary temperature distribution, or something intrinsic to the nature of one or both of Capella's giants? By examining single stars similar to the individual components of Capella (e.g. the Hyades giants for the G8 III component), we should be able to gain a significant insight into this question.

Ayres and Brown (1994), in their analysis of the EUVE spectrum of 31 Com (another likely Hertzsprung gap star), have suggested that the Capella EUVE spectrum (Dupree *et al.* 1993) is really composite, made up of the "flarelike" corona from the more active G0 III secondary (with lines formed at $\approx 10^7$ K, similar to 31 Com), added to the spectrum of the less active G8 III "clump" primary (with lines formed at $\approx 5\times10^6$ K). If this hypothesis is true, then other, post He-flash or "clump" giants should also exhibit a similar DEM as the Capella primary, with line emission at Fe XVIII-Fe XIX dominating the EUV SW spectra. β Cet is one example of this class which has already been observed by EUVE (Ayres *et al.* 1998). However, this picture is complicated by the fact that the 31 Com EUVE spectrum appears to have its peak emission measure at a temperature higher (log T $\approx$ 7.0) than Capella's log T $\approx$ 6.8 "bump" (Dupree *et al.* 1995).

3. Existing X-Ray Observations of the Hyades Giants

3.1 ROSAT All-Sky Survey Data

The ROSAT All-Sky Survey (RASS) observed the four Hyades giants between 1990 July 30 and 1991 January 25: all the giants were detected, with θ^1 and γ Tau being detected at a level roughly 25-50 $\times$ that of δ and ϵ Tau (Stern, Schmitt, and Kahabka 1995). The X-ray fluxes are indicated in Table 1, assuming all the giants at d=45 pc (the X-ray flux differences would be at most 10% changed if we used the proper motion distances indicated in the table). Beacuse of the short exposure time ($<$ 600 s), this data is useful for flux measurements, not spectral modeling.

3.2 ROSAT Pointed Observations

Pye *et al.* (1995) obtained ROSAT PSPC spectra of θ^1 and γ Tau in September 1992. To adequately fit the ROSAT spectra requires at least a 2 temperature (Raymond 1993) model. The model results were, for θ^1 Tau: log T_1 = 6.2, $EM(52)_1$=1.4, log T_2 = 6.9, $EM(52)_2$=3.7, for γ Tau: log T_1= 6.4, $EM(52)_1$= 1.2, log T_2 = 6.8, $EM(52)_2$=1.6 (EM52 = volume emission measure in 10^{52} cm^{-3}).

3.3 ASCA Observations

θ^1 Tau was observed by ASCA from 1344 UT 18 September to 0751 UT 19 September 1995 for a total exposure time of $\approx$ 30 ksec. The count rate in the SIS0 detector was $\sim$ 0.17 counts/sec. No ASCA observations of γ Tau were scheduled. Unlike the very active RS CVn systems, θ^1 Tau exhibits no strong X-ray variability on short or long time scales: the observed SIS count rate is nearly exactly that predicted using the ROSAT PSPC data taken 3 years earlier, and there are no obvious flares

4. EUVE Observations and Analysis

EUVE observed θ^1 Tau for a total of $\approx$ 165 ksec net exposure during the period 21 January to 1 February 1996, and γ Tau for a net exposure of $\approx$ 240 ksec for 7 to 11 February 1997. Spectra were extracted in the SW (70-150 Å) and MW (140-380 Å) bands using the IRAF euv software package (egocs1.6.2; egodata1.13), and the routine "euvextract". The background data for each spectrum was fitted using a 3rd order polynomial function, then the extracted spectra were fitted using a sum of the (then fixed) background spectrum and a multiple gaussian line fitting package developed at LMSAL using IDL. Inputs to the multiple gaussian fitting routine were a series of known strong line locations; the number of line counts, line wavelength, and width were allowed to vary (the latter two within resaoble bounds given the resolution of the SW and MW spectra). In addition, light curves of the DS (Deep Survey) band (70-140 Å) were made for both observations.

5. Results

5.1 EUVE

SW and MW Spectra and Line Fluxes

In Figure 1 (a) we show the results of spectral fitting for θ^1 Tau's SW spectrum, and in Figure 1 (b) a portion of the MW spectrum for the same object. (325–365 Å). The full MW spectrum is not shown, since the region between 140 and 290 Å produced only upper limits, and the region from 290–320 Å is dominated by geocoronal He II 304 Å radiation. In Figure 2 (a) and (b) we show the same results for γ Tau.

In Table 2 we give the line fluxes and upper limits for line emission from θ^1 Tau, and in Table 3 the same information for γ Tau.

5.2 Short and Long Term Variability

The EUVE observations of both θ^1 and γ Tau are perfectly consistent with a constant count rate over $\sim$ 10 (θ^1) and 4 (γ) days (Figures 3 and 4). Earlier ROSAT all sky survey data demonstrated that θ^1 Tau had increased in X-ray luminosity by no more than $\sim$ 50% over the course of a decade (Stern, Schmitt, and Kahabka 1995).

6. Temperature Distribution and Abundances for θ^1 Tau

Given that there is now ASCA data on γ Tau, and the EUVE spectra are of relatively poor S/N quality, we concentrated our modeling efforts on θ^1 Tau. The combined ASCA SIS, GIS and ROSAT data are not adequately fit using a single temperature, solar abundance model (MEKAL or MEKA). Adding a second component improves the fit, but only in the region below 0.5 keV, where only the PSPC is sensitive. However, unlike the case of many active binary systems (e.g. White *et al.* 1994, Antunes *et al.* 1994, Stern *et al.* 1995), which require low (~1/3) Fe abundances, the ASCA fit is improved in the case of θ^1 Tau by allowing the Mg abundance to increase by about a factor of 2 (Mg/H = 1.86±0.25, 90% L.O.C. 1 parameter). However, systematic errors are likely to dominate the error budget, and the reduced χ^2 is only $\sim$ 1.3. Allowing the other elemental abundances to vary seems to have little effect; slight improvements in the fit are gained with a near-zero Ne abundance. The overall fit is shown in Figure 5 (SIS and GIS: top two curves in upper box, PSPC: bottom curve in upper box). Note that the contributions to χ^2 are largely from the SIS data. We have also fit the spectrum to about the same level using a (corrected) Chebyshev polynomial model of the emission measure (EM) distribution (Figure 6). In this case, Mg/H $\sim$ 1.6, showing the systematic effect of changing the temperature distribution. Although we have used the latest released version of SISRSP to generate a customized response matrix for our observation date, allowing the gain to decrease by $\approx$ 2% produces a significant improvement in the fit. Since the SIS data were taken less than 6 months ago, and the latest effects of resolution degradation have not been taken into account in the v0.9 response matrices, this is understandable. There may be other unresolved calibration issues, i.e. near $\approx$ 1 keV.

Combining our ASCA data with ROSAT data taken 3 years previously, we find that the ROSAT 0.5-1.5 keV region is well-fit by the same model used for the ASCA SIS0 data. However, the counts below $\approx$ 0.5 keV in the ROSAT PSPC require the addition of a second component at $\approx$ 0.12 keV.

6.1 DEM Modeling

The EUVE SW and MW spectra for θ^1 Tau clearly shows the presence of line emission from ionization stages Fe XV through XXI. With the EUVE_FIT fitting routine, which uses the sum of terms of an Nth order Chebyshev polynomial to characterize the EM distribution (Stern *et al.* 1995), we find a peaked DEM near log T $\sim$ 6.8. The fitted SW and MW spectra and the derived DEM are shown in Figures 7 and 8 respectively. Note that the region around 304 Å has been removed from the MW spectrum to exclude it from the spectral fit, and that the spectrum extends out to at least 360 Å demonstrating the low column ($N_H < 5 \times 10^{18}$ cm^{-2}) to the Hyades.

7. Summary

All four of the Hyades giants show some evidence of coronal activity, with θ^1 and γ Tau the brightest in X-rays. All observatiuons to date (with EUVE, ASCA, and ROSAT) suggest that these giants are of intermediate activity level compared to the Sun and the very active RS CVn systems. θ^1 Tau, unlike more active RS CVn systems, has a fairly narrow temperature distribution, peaked at log T $\sim$ 6.8. As with β Cet, the Mg/H abundance is enhanced, perhaps by as much as a factor of 2. θ^1 and γ Tau exhibit little of the short term variability seen in active stars, and is relatively constant in X-ray luminosity over several years. The Hyades giants may well be an excellent analog for the G8 III member of the Capella system, accounting for the emission measure "bump" seen in the EUVE spectrum.

8. Acknowledgements

We thank K. Ebisawa, K. Mukai, K. Arnaud, and M. Tripico for much help with the ASCA data analysis, XSPEC models, and FTOOLS Perl problems. EUVE - contract & hospitality of CEA. We also thank S. Drake for supplying a corrected version of K.P Singh's Chebyshev polynomial DEM models for XSPEC. R.A.S. was supported in part by NASA/GSFC contract P.O. S-57777-F and by the Lockheed Martin Independent Research Program.

REFERENCES

Antunes, A., Nagase, F., and White, N.E., 1994, ApJ, 436, L83.

Ayres, T., and Brown, A., 1994, BAAS, 26, 863.

Ayres, T., *et al.* , 1998, ApJ, 496, 428.

Baliunas, S.L., Hartmann, L., and Dupree, A.K., 1983, ApJ, 271, 672.

Baliunas, S.L., *et al.* , 1991, B.A.A.S., 22, 1199.

Brickhouse, N.S., 1995, in IAU Colloq. 152, *Astrophysics in the Extreme Ultraviolet*, eds. S. Bowyer, R. Malina, Kluwer Academic Publishers, p. 105.

Cayrel, R., Cayrel de Strobel, G., Campbell, B., 1985, A&A, 146, 249.

Drake, S.A., Singh, K.P, White, N.E., and Simon, T., 1994S, ApJ, accepted.

Dupree, A.K., Brickhouse, N.S., Doscheck, G.A., Green, J.C., Raymond, J.C., 1993 , ApJ, 418, L41.

Dupree, A.K., Brickhouse, N.S., and Hanson, G.J., 1995, in IAU Colloq. 152, *Astrophysics in the Extreme Ultraviolet*, eds. S. Bowyer, R. Malina, Kluwer Academic Publishers, p. 141.

Eriksson, K., Linsky, J.L., and Simon, T., 1983, ApJ, 272, 665.

Gilroy, K.K., 1989, ApJ, 347, 835.

Griffin, R.F., and Gunn, J.E., 1977, AJ, 82, 176.

Griffin, R.E.M., and Holweger, H., 1989, A&A, 214, 249.

Haisch, B.M., Schmitt, J.H.H.M, and Rosso, C., 1991, ApJ, 383, L15.

Lambert, D.L, and Ries, L.M., 1981, ApJ, 248, 228.

MacDonald, K., *et al.* , 1994, AJ, 108, 1843.

Pilachowski, C.A., and Sowell, J.R., 1992, AJ, 103, 1668.

Pye, J.P., *et al.* , 1995, in preparation.

Ruck, M.J., and Smith, G., 1993, A&A, 277, 165.

Stern, R.A., Schmitt, J.H.M.M., Rosso, C., Pye, J.P., Hodgkin, S.T., and Stauffer, J.R., 1992, ApJ, 399, L159.

Stern, R.A., Lemen, J.R., Pye, J.P., and Schmitt, J.H.M.M., 1995, ApJ, 444, L45.

Stern, R.A., Schmitt, J.H.M.M., and Kahabka, 1995, ApJ, 448, 683.

White, N.E., *et al.* , 1994, PASJ, 46, L97.

Table 1: Hyades Giants – Chromospheric, Transition Region and Coronal Luminosities

Star	V	V-R	Sp Type	d (pc)	Mg h+k	O I	Si II	Si IV	C IV	N V	X-Ray
γ *Tau*	3.65	0.73	K0 IIIab	45.2	480.	9.4	6.0	2.1	1.7	3.6	66.
θ^1 *Tau*	3.83	0.71	K0 IIIb	46.2	430.	8.8	17.	3.8	3.8	1.7	130.
δ *Tau*	3.76	0.73	K0 III	47.7	270.	5.0	5.7	<0.7	<0.7	<0.5	≈ 4
ϵ *Tau*	3.54	0.73	G9.5 III	45.7	285.	5.0	2.0	<1.	<0.7	<1.	≈ 2

[Note: all luminosities in units of 10^{28} erg s^{-1}. Hyades data from Baliunas, Hartmann and Dupree (1983), Zolcinski *et al.* (1983), Caillault, Vilhu and Linsky (1991) and Stern, Schmitt, and Kahabka (1995); distances from Patience *et al.* (1998) (Schwan 1991 values multiplied $\times$ 0.966 from Hipparchos ditance scale results of Perryman *et al.* (1998)].

Table 2: EUVE Line Fluxes: θ^1 Tau

Ion	λ_{lab}	λ_{fit}	Width	Flux[1]
Ne VII	89.40	89.38± 0.06	0.23± 0.06	< 0.026
Fe XVIII	93.90	93.95± 0.03	0.21± 0.03	0.056± 0.018
Ne VIII?	98.30	98.26± 0.04	0.21± 0.04	0.027± 0.014
Fe XXI	102.20	102.20± 0.04	0.23± 0.03	0.021± 0.013
Fe XVIII	103.90	103.88± 0.04	0.21± 0.04	0.034± 0.015
Fe XIX	108.40	108.38± 0.03	0.22± 0.03	0.044± 0.015
Fe XXII	114.40	114.34± 0.05	0.21± 0.05	0.013± 0.015
Fe XXII	117.20	117.18± 0.05	0.23± 0.04	< 0.026
Fe XX	118.70	118.76± 0.06	0.21± 0.06	< 0.030
Fe XX	121.80	121.84± 0.04	0.21± 0.04	0.024± 0.017
Fe XXI	128.70	128.76± 0.05	0.23± 0.05	0.004± 0.019
Fe XXIII/XX	132.90	132.89± 0.04	0.21± 0.03	0.051± 0.025
Fe XXII	135.80	135.81± 0.05	0.21± 0.04	0.024± 0.024
Fe XVI	335.40	335.36± 0.06	0.50± 0.05	0.306± 0.063
Fe XVI	360.80	360.80± 0.09	0.60± 0.09	0.028± 0.034

[[1] All fluxes in units of 10^{-3} ph cm^{-2} s^{-1}. Errors are 1σ except for fluxes = 0, where 2σ upper limits are given].

Table 3: EUVE Line Fluxes: γ Tau

Ion	λ_{lab}	λ_{fit}	Width	Flux[1]
Ne VII	89.40	89.42$\pm$ 0.03	0.23$\pm$ 0.03	$<$ 0.030
Fe XVIII	93.90	93.92$\pm$ 0.03	0.21$\pm$ 0.03	0.044$\pm$ 0.017
Ne VIII?	98.30	98.29$\pm$ 0.03	0.21$\pm$ 0.03	0.014$\pm$ 0.014
Fe XXI	102.20	102.20$\pm$ 0.03	0.21$\pm$ 0.03	$<$ 0.027
Fe XVIII	103.90	103.88$\pm$ 0.03	0.22$\pm$ 0.03	0.014$\pm$ 0.014
Fe XIX	108.40	108.39$\pm$ 0.03	0.21$\pm$ 0.02	0.031$\pm$ 0.015
Fe XXII	114.40	114.40$\pm$ 0.03	0.25$\pm$ 0.03	$<$ 0.027
Fe XXII	117.20	117.20$\pm$ 0.03	0.21$\pm$ 0.02	0.031$\pm$ 0.017
Fe XX	118.70	118.65$\pm$ 0.03	0.21$\pm$ 0.04	$<$ 0.034
Fe XX	121.80	121.82$\pm$ 0.03	0.24$\pm$ 0.03	$<$ 0.030
Fe XXI	128.70	128.67$\pm$ 0.03	0.25$\pm$ 0.04	$<$ 0.038
Fe XXIII/XX	132.90	132.89$\pm$ 0.03	0.21$\pm$ 0.02	0.055$\pm$ 0.026
Fe XXII	135.80	135.76$\pm$ 0.03	0.21$\pm$ 0.03	0.016$\pm$ 0.026
Fe XVI	335.40	335.31$\pm$ 0.06	0.57$\pm$ 0.06	0.069$\pm$ 0.044
Fe XVI	360.80	360.72$\pm$ 0.07	0.45$\pm$ 0.07	$<$ 0.094

[[1] All fluxes in units of 10^{-3} ph cm^{-2} s^{-1}. Errors are 1σ except for fluxes = 0, where 2σ upper limits are given].

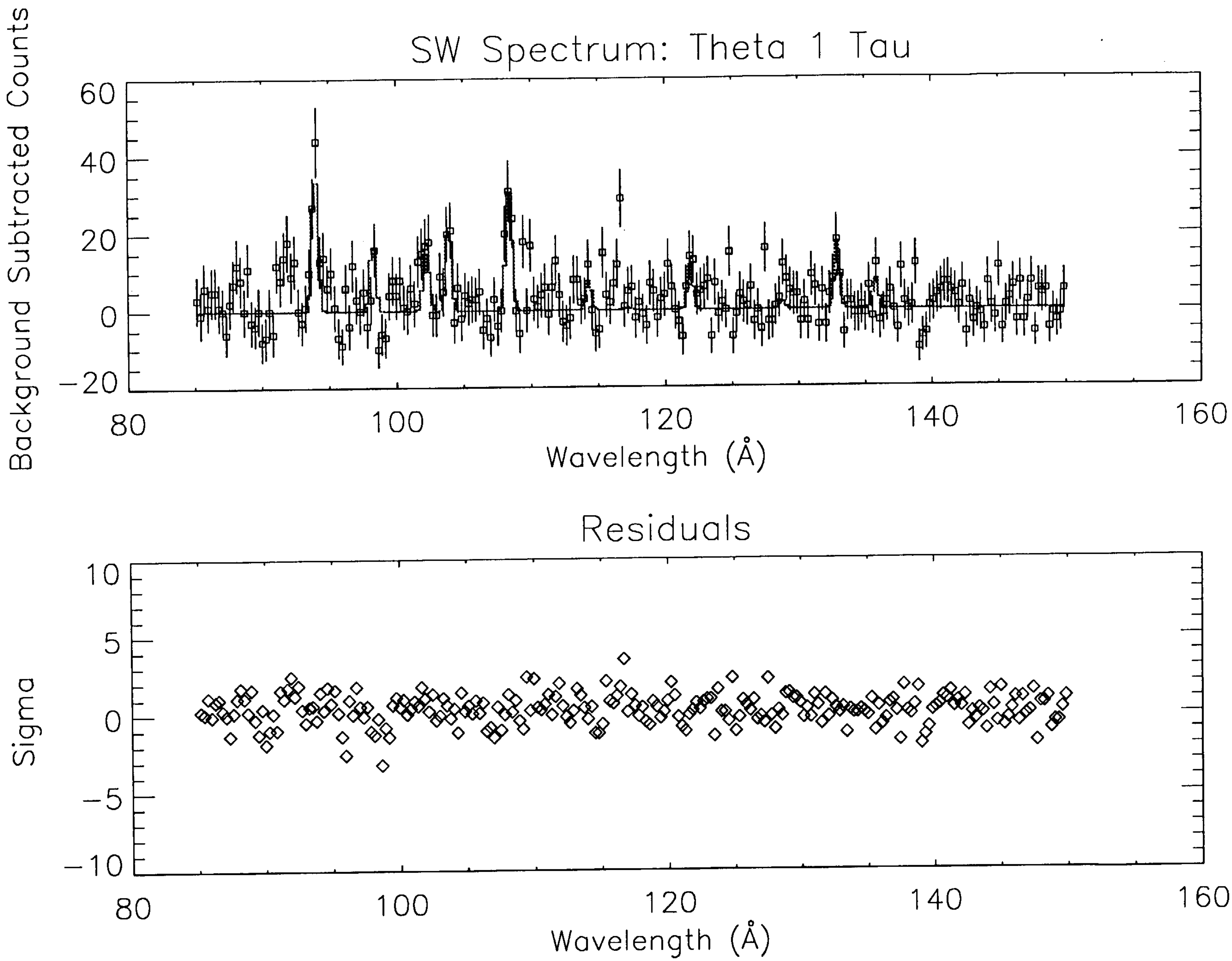

SW Spectrum: Theta 1 Tau
Background Subtracted Counts
60
40
20
0
−20
80
100
120
140
160
Wavelength (Å)
Residuals
Sigma
10
5
0
−5
−10
80
100
120
140
160
Wavelength (Å)

FIGURE 1(a)

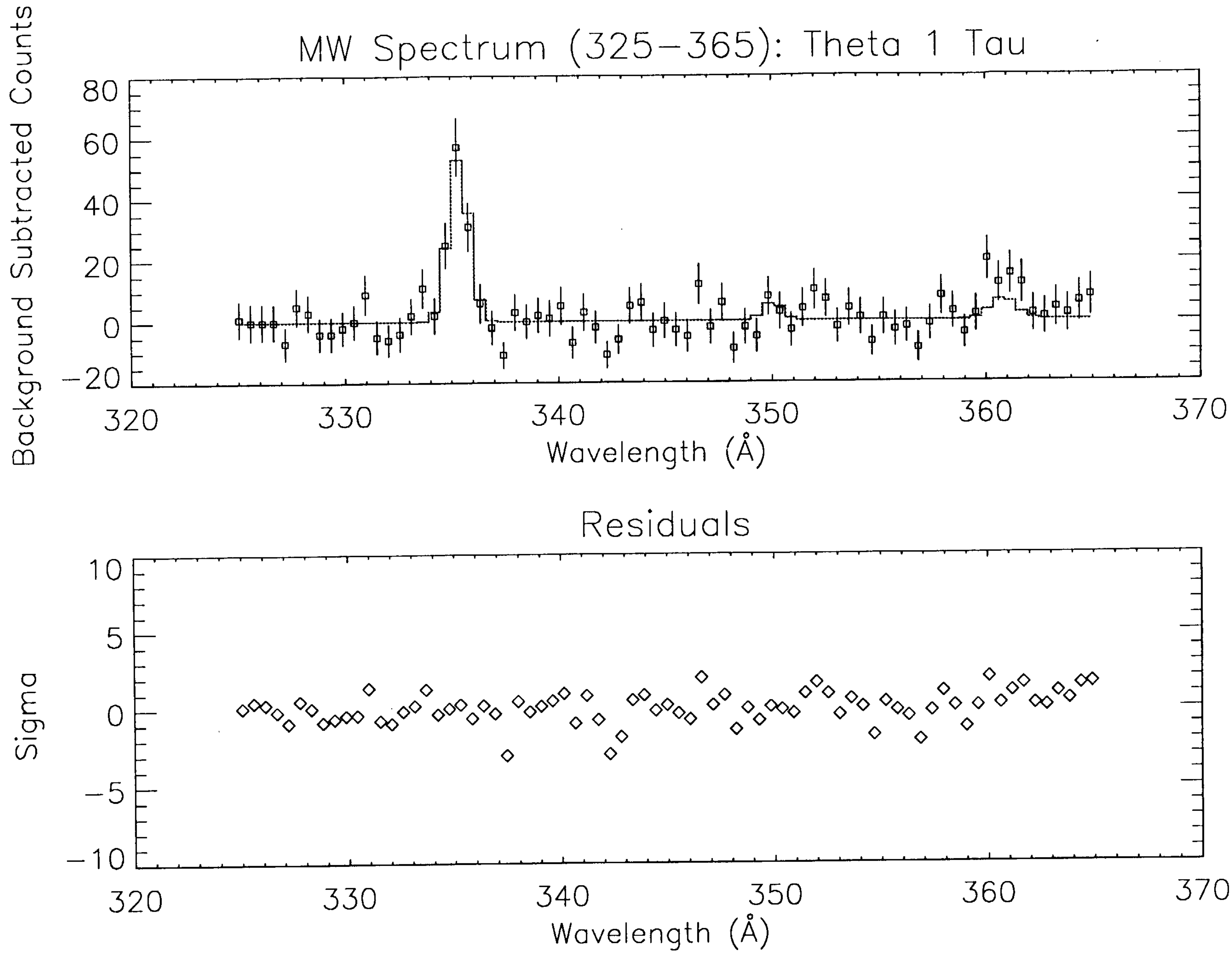
MW Spectrum (325–365): Theta 1 Tau
Background Subtracted Counts
80
60
40
20
0
−20
320
330
340
350
360
370
Wavelength (Å)
Residuals
Sigma
10
5
0
−5
−10
320
330
340
350
360
370
Wavelength (Å)

Figure 1(b)

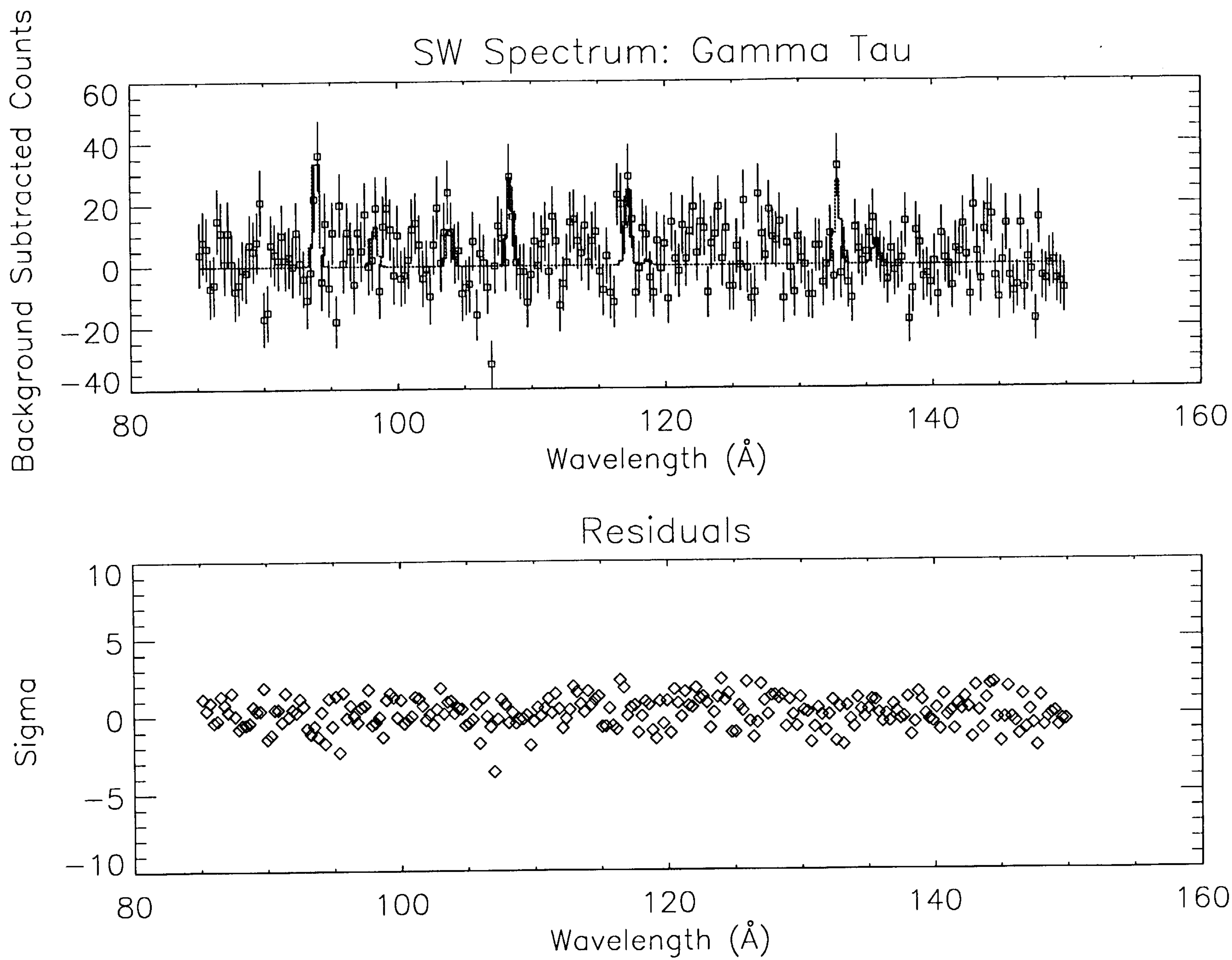
SW Spectrum: Gamma Tau
Background Subtracted Counts
60
40
20
0
−20
−40
80
100
120
140
160
Wavelength (Å)
Residuals
Sigma
10
5
0
−5
−10
80
100
120
140
160
Wavelength (Å)

Figure 2(a)

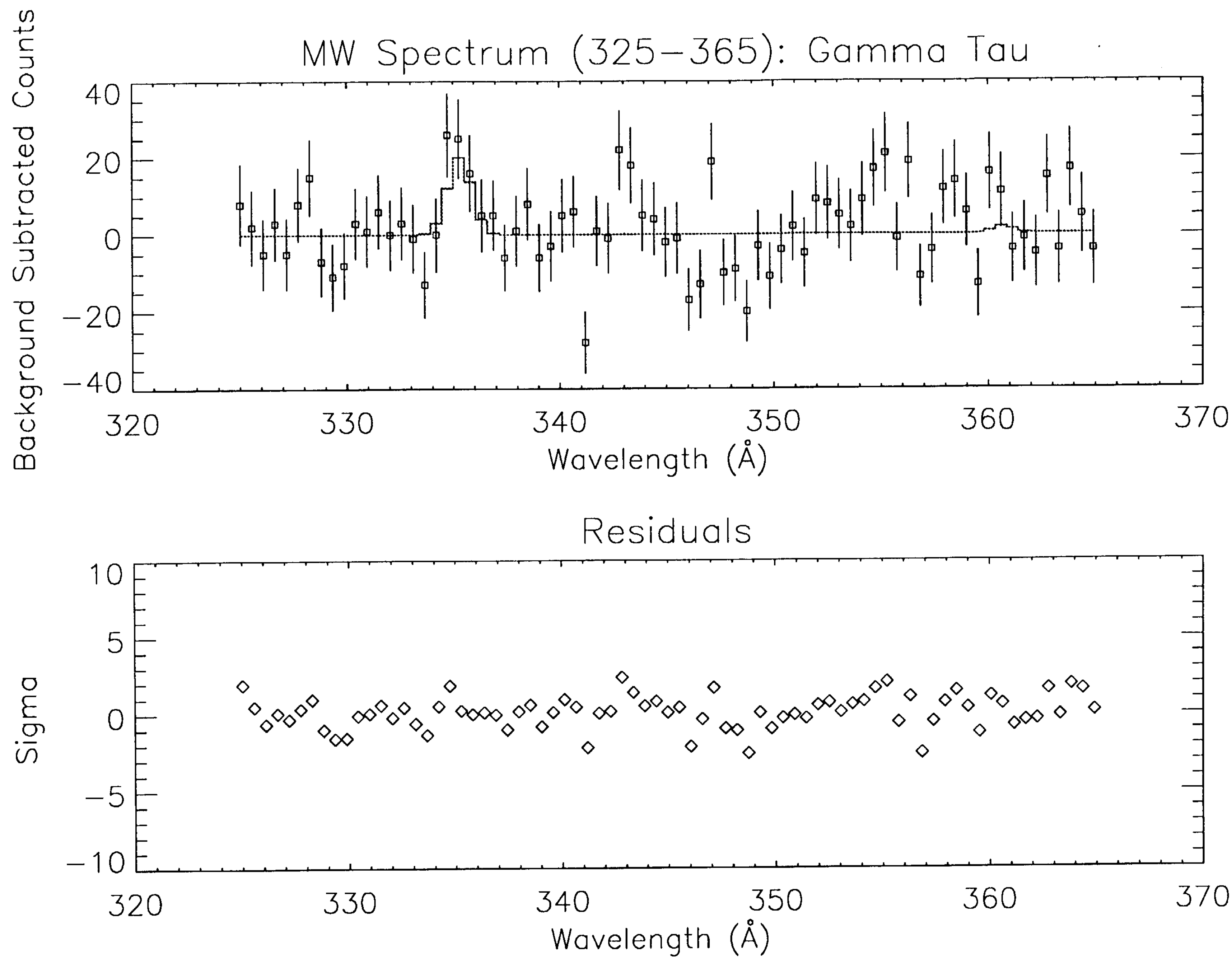
MW Spectrum (325–365): Gamma Tau
Background Subtracted Counts
40
20
0
−20
−40
320
330
340
350
360
370
Wavelength (Å)
Residuals
Sigma
10
5
0
−5
−10
320
330
340
350
360
370
Wavelength (Å)

Figure 2(b)

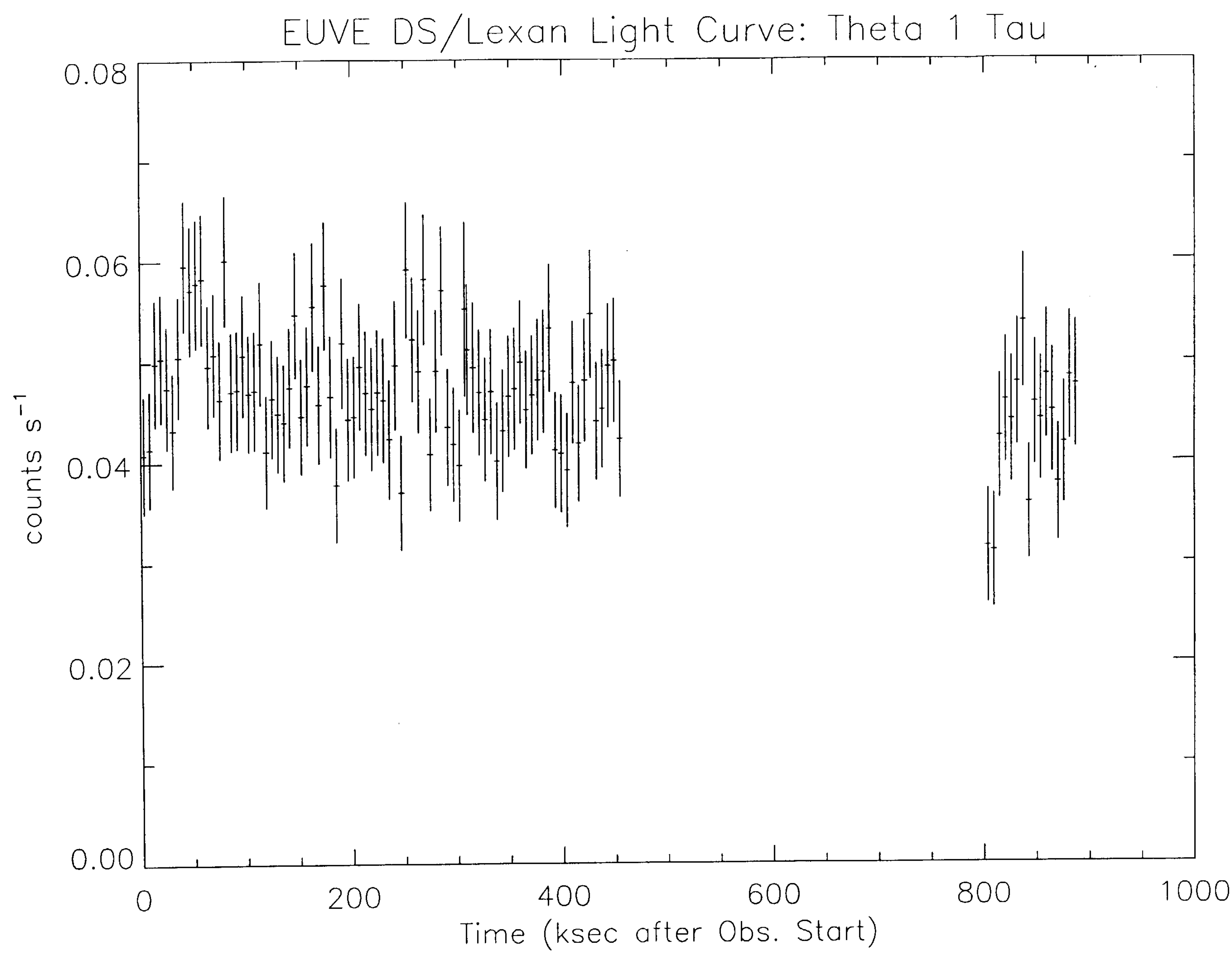
EUVE DS/Lexan Light Curve: Theta 1 Tau
0.08
0.06
0.04
0.02
0.00
counts s^{-1}
0
200
400
600
800
1000
Time (ksec after Obs. Start)

FIGURE 3

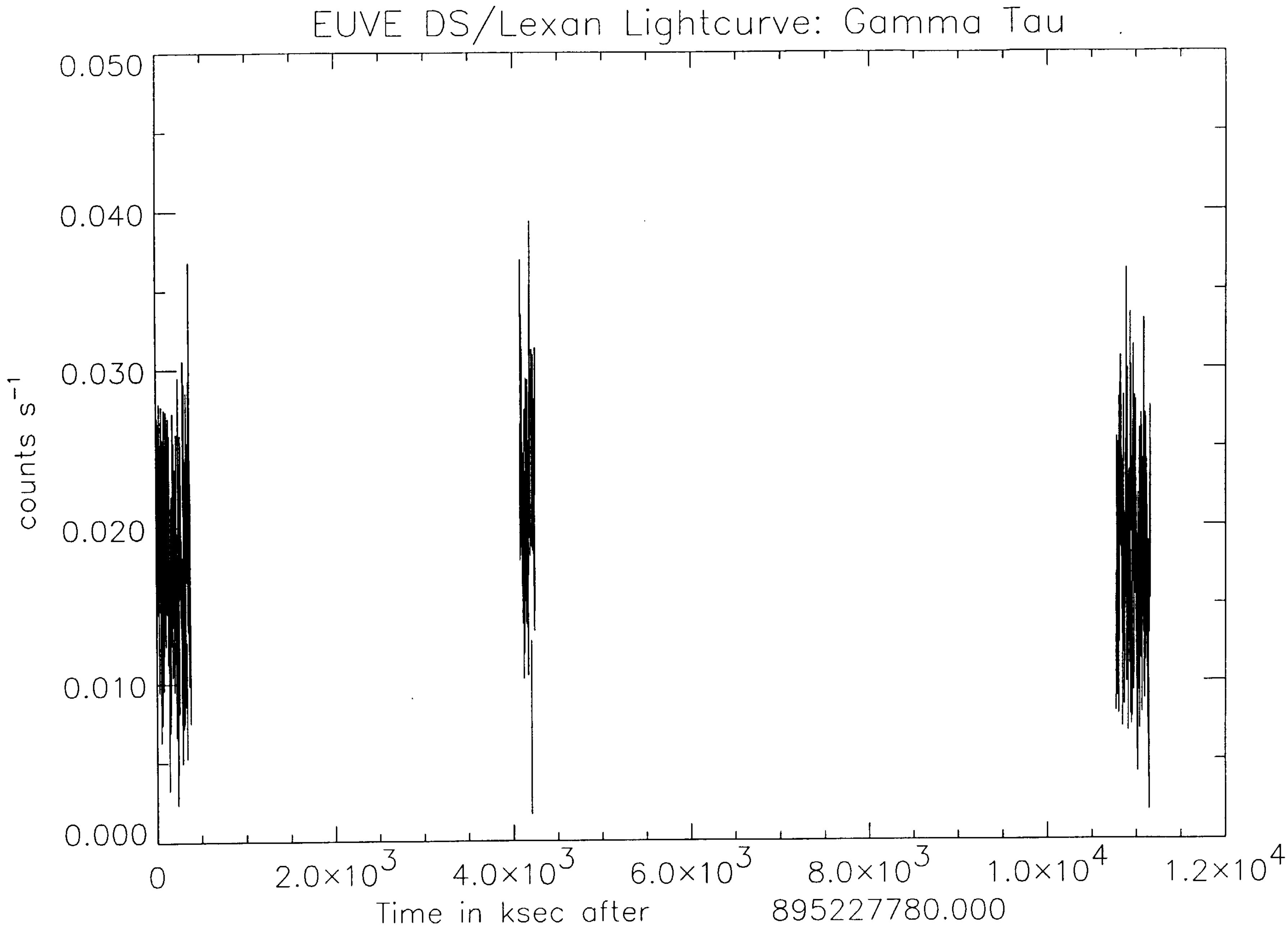

EUVE DS/Lexan Lightcurve: Gamma Tau
counts s^{-1}
0.050
0.040
0.030
0.020
0.010
0.000
0
2.0×10^3
4.0×10^3
6.0×10^3
8.0×10^3
1.0×10^4
1.2×10^4
Time in ksec after 895227780.000

FIGURE 4

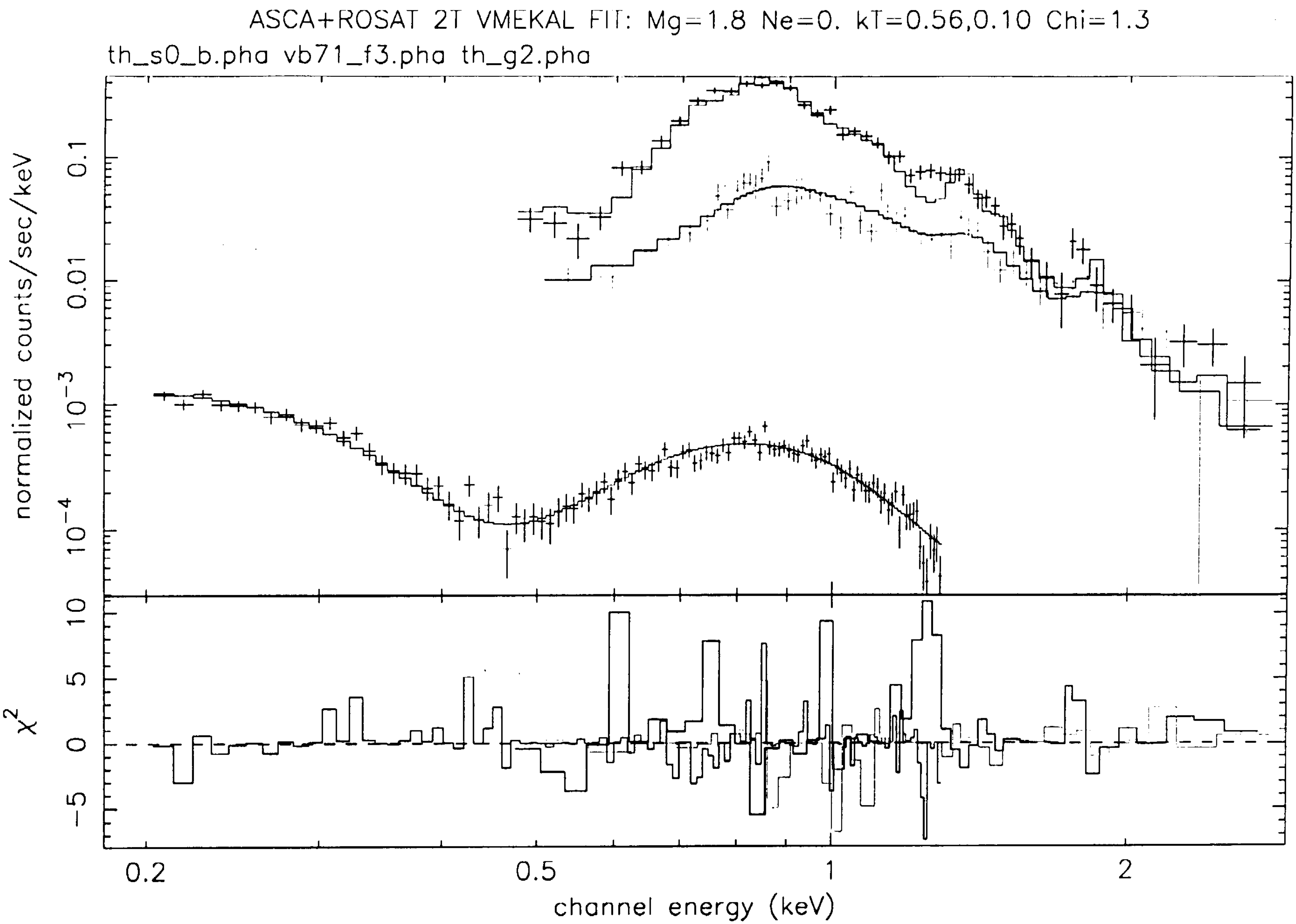
ASCA+ROSAT 2T VMEKAL FIT: Mg=1.8 Ne=0. kT=0.56,0.10 Chi=1.3
th_s0_b.pha vb71_f3.pha th_g2.pha
normalized counts/sec/keV
0.1
0.01
10^-3
10^-4
χ^2
10
5
0
−5
0.2
0.5
1
2
channel energy (keV)

FIGURE 5

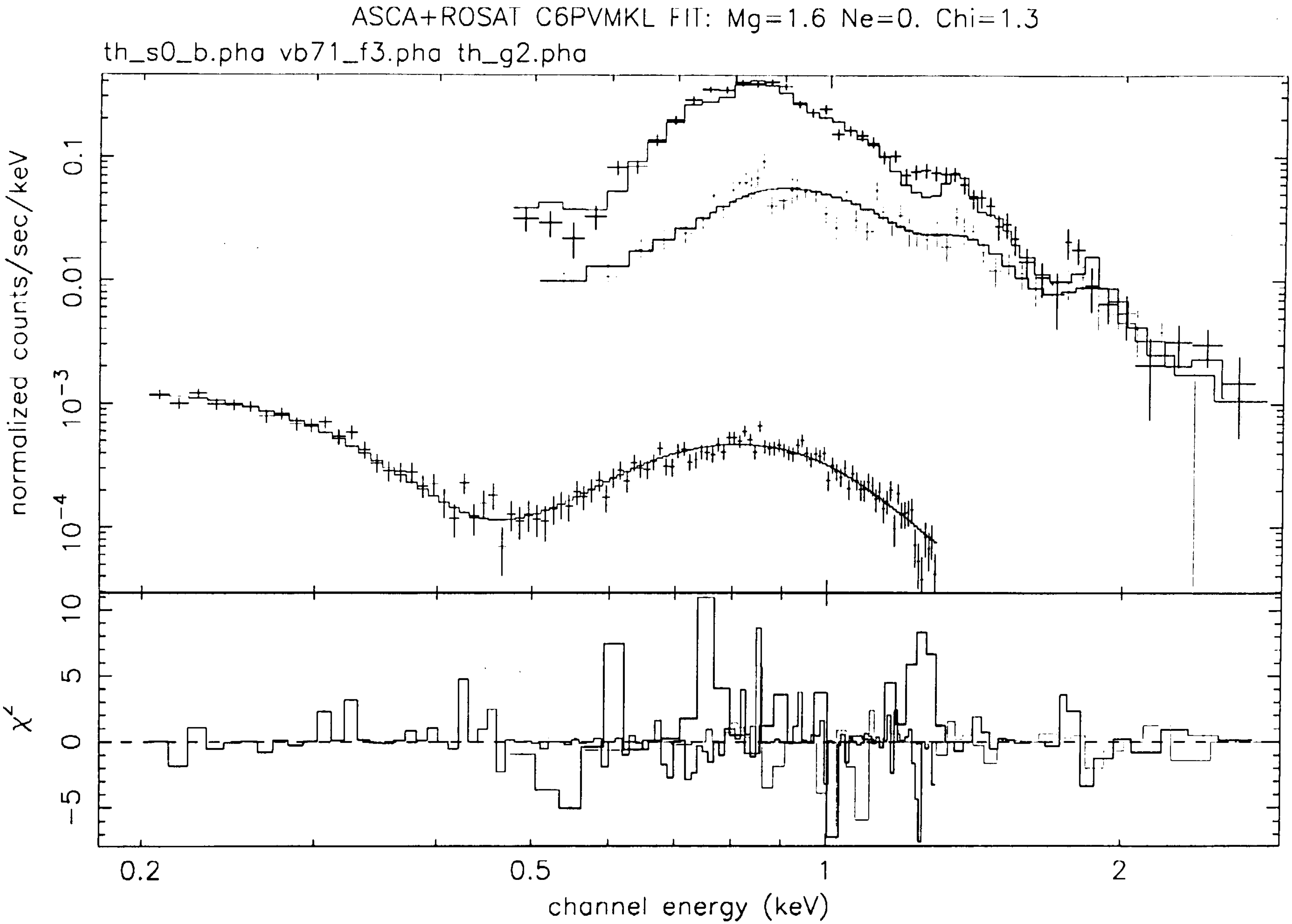
ASCA+ROSAT C6PVMKL FIT: Mg=1.6 Ne=0. Chi=1.3
th_s0_b.pha vb71_f3.pha th_g2.pha
normalized counts/sec/keV
0.1
0.01
10^{-3}
10^{-4}
χ^2
10
5
0
−5
0.2
0.5
1
2
channel energy (keV)

FIGURE 6

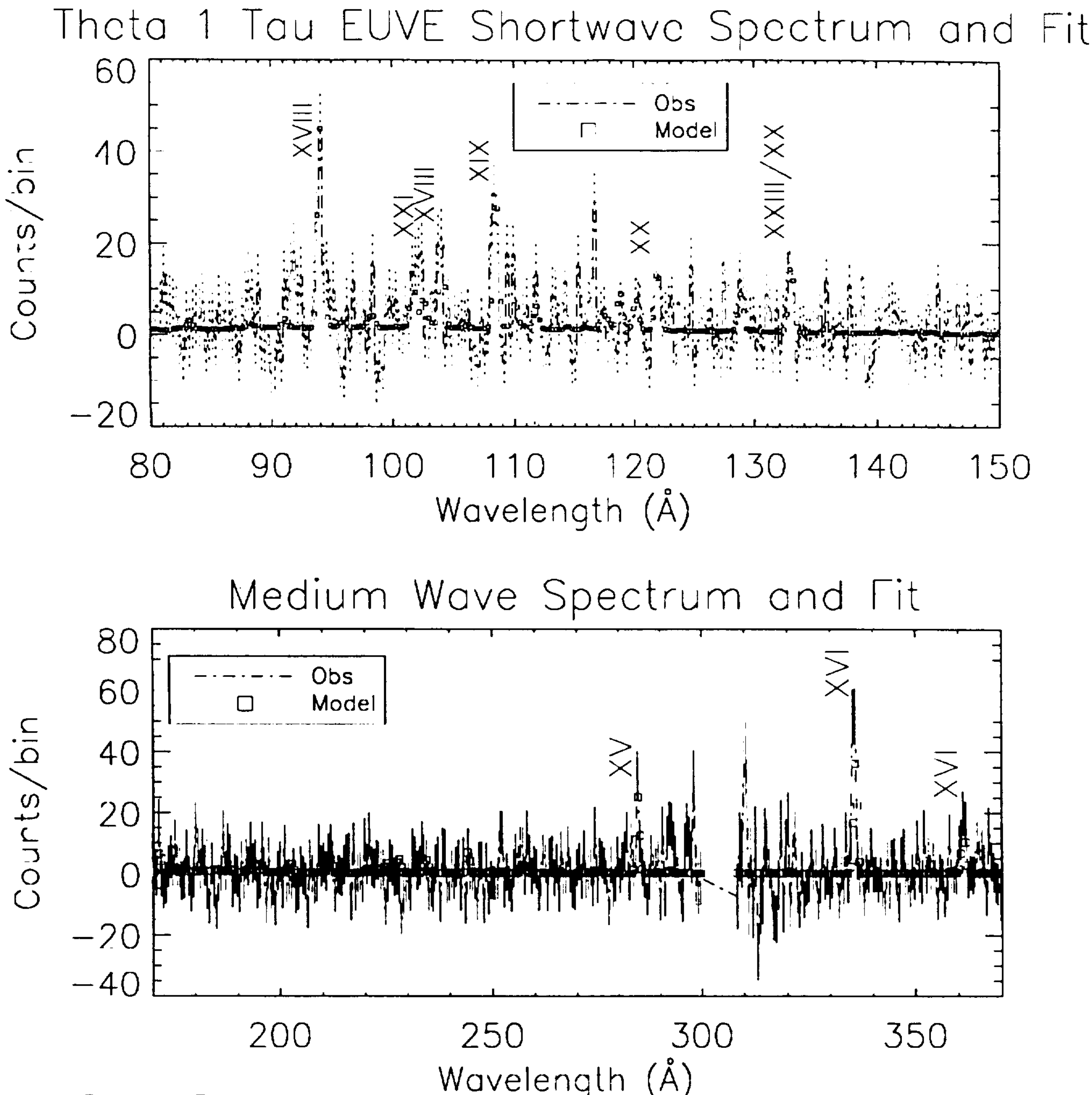
Theta 1 Tau EUVE Shortwave Spectrum and Fit
Obs
Model
Counts/bin
Wavelength (Å)
XVIII
XXI
XVIII
XIX
XX
XXIII/XX
Medium Wave Spectrum and Fit
Obs
Model
Counts/bin
Wavelength (Å)
XV
XVI
XVI

FIGURE 7

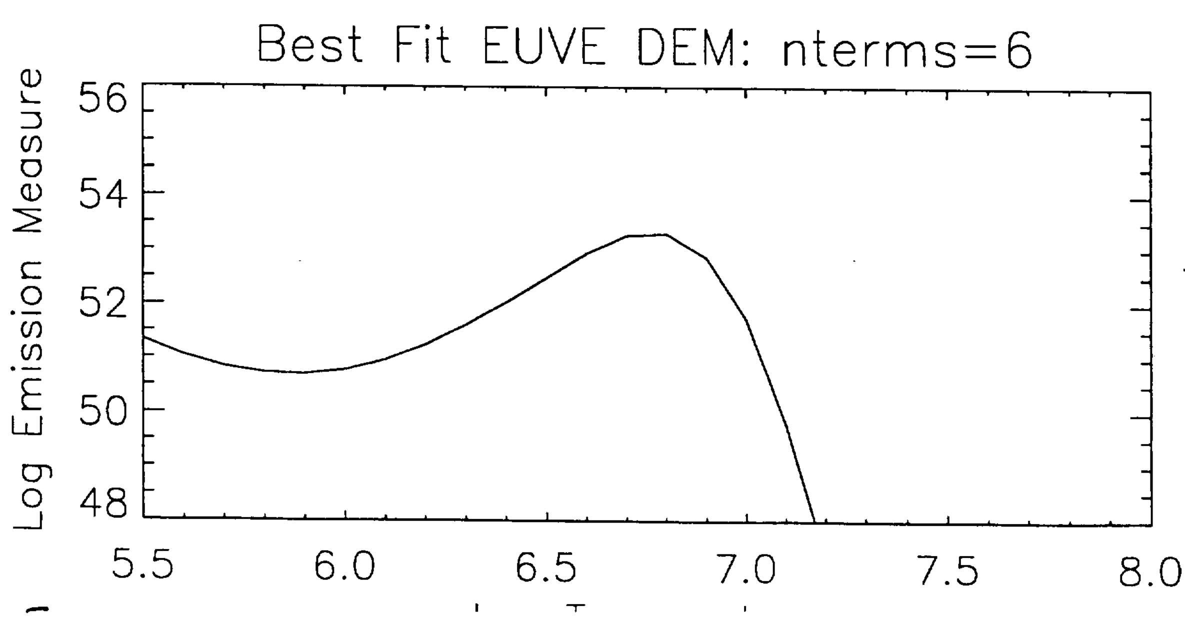
Best Fit EUVE DEM: nterms=6
Log Emission Measure

REPORT DOCUMENTATION PAGE

Form Approved
OMB No. 0704-0188

1. AGENCY USE ONLY *(Leaveblank)*	2. REPORT DATE	3. REPORT TYPE AND DATES COVERED
	30 Sep 1998	Final Report 10/97-9/98

4. TITLE AND SUBTITLE EUVE Observations of the Hyades Giants

5. FUNDING NUMBERS
Contract P.O. S-92503-Z

6. AUTHORS
Robert Stern

7. PERFORMING ORGANIZATION NAME(S) AND ADDRESS(ES)
Lockheed Martin Missiles & Space
Advanced Technology Center
3251 Hanover Street, H1-12/252
Palo Alto, CA 94304-1191

8. PERFORMING ORGANIZATION REPORT NUMBER
GBS-98-203

9. SPONSORING/MONITORING AGENCY NAME(S) AND ADDRESS(ES)
NASA Goddard Space Flight Center
Space Sciences Procurement Office Code 216
Greenbelt, MD 20771

10. SPONSORING/MONITORINGAGENCY REPORT NUMBER

11. SUPPLEMENTARYNOTES

12a DISTRIBUTION/AVAILABILITYSTATEMENT

12b. DISTRIBUTION CODE

13. ABSTRACT *(Maximum 200 words)*

We describe EUVE and ROSAT observations of the Hyades K0 III giants θ^1 (vB 71=HR1411) and γ (vB 28=HR1346) Tau. We also discuss ASCA observations of θ^1 Tau. The coronal activity of these ``clump" giants is intermediate between that of the Sun and of high activity stars such as RS CVn systems. There is no evidence for significant short or long term variability up to several years. Modeling of the individual and combined spectra suggest that these two X-ray and EUV-bright Hyades giants resemble in their activity levels another clump giant, β Cet, with a peak in the emission measure distribution near log T $\sim$ 6.8, reminiscent of the Capella emission measure ``bump."

14. SUBJECT TERMS
coronae;ultraviolet;stars

15. NUMBER OF PAGES
21

16. PRICE CODE

17. SECURITY CLASSIFICATION OF REPORT	18. SECURITY CLASSIFICATION OF THIS PAGE	19. SECURITY CLASSIFICATION OF ABSTRACT	20. LIMITATION OF ABSTRACT
Unclassified	Unclassified	Unclassified	